Permanent Magnets for MEMS

David P. Arnold, *Member, IEEE*, and Naigang Wang, *Student Member, IEEE*

***Abstract*—This paper reviews the state of the art for the microfabrication of permanent magnets applicable to microelectromechanical systems (MEMS). Permanent magnets are a key building block for the realization of magnetically based MEMS sensors, actuators, and energy converters. In this paper, the basic theories and operational concepts for permanent magnets are first described. Then, different classes of permanent-magnet materials and associated performance tradeoffs are introduced. Challenges relating to the integration of permanent magnets into MEMS applications are then discussed. Last, a summary and review of previously reported fabrication strategies and material properties is provided. [2009-0179]**

***Index Terms*—Magnetic alloys, magnetic devices, magnetic microactuator and system (MAGMAS), magnets, microelectromechanical systems (MEMS), microfabrication.**

I. Introduction

PERMANENT or "hard" micromagnets are a critical enabling component for the development of high-performance microscale magnetic machines such as motors, generators, switches, pumps, acoustic speakers, and energy harvesters. Permanent magnets are ferromagnetic or ferrimagnetic materials that exhibit a strong magnetization in the absence of an external magnetic field. Once magnetized, they provide a "free" source of magnetic fields, requiring no external power. In contrast, soft magnets only become magnetized in the presence of an external magnetic field, from either a current-carrying wire or a permanent magnet. Hard magnets are often coupled with soft magnetic cores to guide and concentrate magnetic fields in specific regions, e.g., across coils for an electrodynamic actuator.

An analysis of physical scaling laws reveals the importance of permanent magnets for microscale applications [1]. Magnetic fields from a current-carrying electromagnet unfavorably scale with diminishing size, whereas the fields from a permanent magnet are scale invariant, at least down to a certain point. The source of magnetic fields in an electromagnet is the current, which, in a nonsuperconducting material, is a dissipative process and, thus, thermally limited. This sets a practical limit on the suitability of microcoils for generating magnetic fields via electrical currents. In contrast, the source of magnetic fields in a permanent magnet is residual material magnetization, which arises at the atomic level. A large magnet and a small magnet possess the same magnetization and thus are capable of producing similar external magnetic field strengths. This scaling is fairly constant down to the size scale of a single domain (usually < 100 nm). Below this size (usually < 10 nm), thermal energy can dominate, and the magnet may exhibit a superparamagnetic behavior with no residual magnetization [2]. Above this nanoscale limit, however, permanent magnets provide an effective means for realizing strong static magnetic fields in microscale devices.

While hard magnets have been known for thousands of years, it was only in the late twentieth century that the fundamental understanding of magnetism and magnetic materials led to advancements in their magnetic properties. Today, high-performance permanent magnets are ubiquitous in many different macroscale systems such as motors, generators, loudspeakers, latching mechanisms, cathode ray tubes, scientific instruments, and toys. However, the application of permanent magnets at the microscale has fairly been limited, with the notable exception of magnetic recording media.

The methods for magnet fabrication at the macroscale, i.e., casting and powder processing, are starkly foreign to traditional thin-film microfabrication approaches, i.e., physical vapor deposition, chemical vapor deposition, and electrochemical deposition. While there is a wealth of information on both soft and hard magnetic thin films as it relates to magnetic media [3], [4], these films are too thin (often less than 100 nm) to be applicable for most magnetic microelectromechanical systems (MEMS). For example, it has been argued that magnetic actuators are more favorable than electrostatic actuators when the actuation gap is greater than ~ 2 μm [5]. This implies the need for relatively voluminous (thick) magnetic structures to establish reasonably strong magnetic fields over multimicrometer-length scales.

Over the past decades and heavily borrowing from the techniques used for magnetic recording read/write heads [6], soft magnets have readily been adopted by the MEMS community. Sputtering, evaporation, and electroplating have been used to form microstructures of soft Ni, Fe, and Co alloys [7], [8], enabling a host of sensors, actuators, and micromachines [9]. Certain properties of these soft magnetic films, particularly the permeability and coercivity, are often much lower than those found in bulk, but these inadequacies have not hampered their utility. This is because the overall system performance has often been limited by other design/fabrication issues (e.g., current density limits, air gap control, mechanical flexures, and complex fabrication).

The application and integration of hard magnets in MEMS present even more design and fabrication challenges.

1) Unlike soft magnetic films, there is no preexisting knowledge base from which to draw. The need for relatively

Manuscript received July 17, 2009; revised September 13, 2009. First published November 10, 2009; current version published December 1, 2009. This work was supported in part by the National Science Foundation under Grant DMI-0556056 and Grant ECCS-0716139. Subject Editor C. H. Ahn.

The authors are with the University of Florida, Gainesville, FL 32611 USA (e-mail: darnold@ufl.edu).

Color versions of one or more of the figures in this paper are available online at http://ieeexplore.ieee.org.

Digital Object Identifier 10.1109/JMEMS.2009.2034389

thick films of hard magnetic materials is somewhat unique to MEMS applications.

2) Like soft magnets, there are different classes of hard magnetic materials, each with strengths and weaknesses. The magnetic performance, temperature effects, chemical stability, and fabrication constraints all play a role in the material selection and microfabrication strategy.
3) The material properties of most hard magnets are typically quite sensitive to both the microstructure and the chemical composition. This requires careful control over the processing conditions and may require the application of magnetic fields, additional thermal steps, or other processing steps to induce optimal magnetic properties, thus adding cost and complexity to the fabrication.
4) Hard magnets require *in situ* or postfabrication magnetization steps to "pole" the magnets in a specific direction. This complicates the integration process, particularly for wafer-scale batch fabrication. It also usually implies that all magnets on a wafer are magnetized in only one direction, which restricts the device design.
5) Perhaps most importantly, the total system performance of a permanent-magnet-based system is usually limited by the magnet. Thus, the quality and performance of the magnetic material play a critical role in the overall design.

The purpose of this paper is to: 1) briefly review the basics of permanent magnetic materials to provide a foundation for discussion; 2) describe the interplay between the fabrication, microstructure, and material properties of common hard magnetic materials; 3) highlight the challenges for achieving relatively thick ($> 1\ \mu$m) high-performance integrable permanent magnets via microfabrication; and 4) catalog, summarize, and review the recent progress in this area.

This paper updates and expands a previous review by Chin in 2000 [10]. At the time of Chin's assessment, many of the reviewed materials had low performance, were not suitable for MEMS integration, or were early concepts borrowed from other applications. Since then, tremendous progress has been made on the development of permanent-magnet materials, specifically intended for MEMS applications. Thus, another goal of this paper is to help catalyze the ongoing development of micromagnetic sensors, actuators, and systems.

II. Material Properties for Magnets

This section describes the important material properties for hard ferromagnetic materials from an engineering perspective. For design purposes, the most relevant engineering properties are the magnetic properties (intrinsic coercivity, coercivity, remanence, and maximum energy product), the thermal properties (Curie temperature, maximum operating temperature, and temperature coefficient of remanence), and the chemical stability. The definitions of these properties and their significance are well known by the magnetics community. They are briefly reviewed below to familiarize those in the MEMS community who want to employ magnets for microsystem design but are not intimately familiar with the terminology or details of magnetic materials. Unfortunately, magnetism and magnetic materials are often employed but not well understood. More thorough treatments of these topics can be found in [2] and [11]–[14].

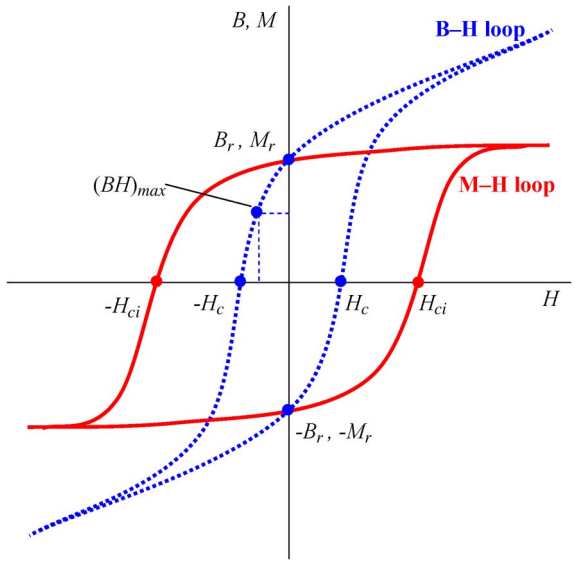

Fig. 1. M–H and B–H magnetic hysteresis loops.

A. Basic Magnetic Theory

The macroscopic magnetic behavior of a ferromagnet is widely recognized by its magnetic hysteresis loop, which is shown in Fig. 1. This complex behavior is the result of microscale and atomic-scale physical phenomena within the material, and various theories have been developed to describe and model this behavior. In the localized moment theory [11], each atom is assumed to possess a small vector magnetic moment. The total magnetic moment of a magnet is the superposition (vector sum) of all the atomic moments that comprise the magnet. Dividing this total magnetic moment by the volume of the region yields the magnetization, which is denoted M. The magnetization is a vector field quantity describing the magnetic moment density.

A strong magnetization arises when individual atomic moments align in a given direction. In ferromagnetic materials, this spontaneously occurs, due to an interatomic coordination known as exchange interaction. Groups of atoms (typically clusters of $10^{17}-10^{21}$ atoms [12]) band together to form distinct regions known as magnetic domains. Domains may point in different directions, but each has a strong material-dependent magnetization. The domains in a magnet organize in a manner to minimize the total energy. This energy minimization process tends to align the magnetic domains in certain directions, depending on the crystalline axes and physical shape (both macroscopic and microstructural). This is important, because the ability to control the crystalline structure/orientation and microstructural particle/grain shape is critical for realizing strong magnets. This is also one origin of the hysteretic behavior of a magnet.

B. Magnetic Properties

There are three vector fields that define the state of a magnet: the magnetic flux density $\vec{B}$, the magnetic field $\vec{H}$, and the

magnetization $\vec{M}$. At any given point, these field quantities are related by the constitutive equation $\vec{B} = \mu_0(\vec{H} + \vec{M})$, where $\mu_0 = 4\pi \times 10^{-7}$ H/m is the permeability of free space. In a ferromagnet, the magnetization is a nonlinear and hysteretic function of the magnetic field, resulting in complex material relationships. Fundamentally, this behavior is governed by the physical rearrangement of the magnetic domains under an applied field.

For design purposes, this phenomenon is quantified by an experimentally measured magnetic hysteresis M–H curve, which is depicted in Fig. 1. This curve, which is actually a multivalued "loop," describes how a magnet is magnetized/demagnetized with a varying magnetic field H. An equivalent B–H loop can be derived from the M–H loop via the constitutive equation, and vice versa. These two plots have slightly different appearance and interpretation but convey similar information. Material scientists and physicists usually focus on the M–H loop, while engineers tend to prefer the B–H loop.

One confusing aspect is the magnetic field in the constitutive equation, and depicted in Fig. 1 is the total internal field $H = H_{\rm tot} = H_a + H_d$, where H_a is an externally applied field, and H_d is an internally generated demagnetizing field. In any finite-length magnet, a demagnetizing field arises because of the free magnetic poles at the terminating ends of the magnet. This strength of the field is dependent on the magnetization and the physical magnet shape; furthermore, it acts in a direction opposite to the magnetization, essentially acting to demagnetize the magnet. The demagnetizing field is generally expressed as $H_d = -N_d M$, where N_d is the demagnetization factor. Values for N_d can be found in [11] and other magnetic references.

The important ramification of this demagnetizing field is that when a permanent magnet is used as a source of magnetic flux, its operating point is somewhere in the second quadrant of the hysteresis loop; the internal magnetic field H is actually in opposite direction to the magnetic flux density B and magnetization M. This second-quadrant portion of the hysteresis loop, which is known as the demagnetization curve, provides the critical information necessary for magnetic design.

The key features of the hysteresis loop for a permanent magnet are depicted in Fig. 1 and described as follows. The intrinsic coercivity H_{ci} is the reversal magnetic field required to force the magnetization to zero. The coercivity H_c is similarly the reversal magnetic field required to force the magnetic flux to zero. Note that the intrinsic coercivity is usually substantially larger than the coercivity for most permanent magnets. Furthermore, note that many authors use the term "coercivity" when "intrinsic coercivity" is really the intent. Careful attention should be paid for accurate interpretation. Practically speaking, the coercivity values indicate how hard it is to magnetize or demagnetize the magnet, with larger coercivities preferred.

In contrast, the remanence B_r indicates how strong a magnet is, once magnetized. More specifically, B_r is the maximum magnetic flux density that the magnet can provide. This maximum value is only achieved when the total internal magnetic field is zero. For a simple magnet, this specific condition is only met if the end poles of the magnet are "short-circuited" by a highly permeable magnetic structure, thus eliminating all internal demagnetizing fields. However, in this configuration, the magnetic fields are completely contained within the magnetic structures (no air gaps), so this is of limited practical use, except perhaps for latching-type structures.

While the coercivities and remanence indicate theoretical material limits, the normal operating point for a magnet is somewhere in between these bounds. For instance, for a simple magnet in free space, the B-fields near the pole surfaces are usually only 20%–50% of B_r. The product of B and H has units of energy density, in kilojoules per cubic meter. The maximum energy density product $(BH)_{\max}$ is the operating point where the product $|B \cdot H|$ is maximized in the second quadrant. This value represents an operating point where the magnet can supply the most magnetic energy to an air gap, which is particularly important for actuator applications [13]. As such, the maximum energy product (often termed "energy product" for conciseness) is often used as the primary figure of merit for comparison of hard magnetic materials. It should be noted, however, that for devices where a large static magnetic field is required, this may not be the best indicator of performance; the (intrinsic) coercivity or remanence may serve as better figures of merit.

C. Thermal Properties

The performance of a permanent magnet is highly dependent on temperature, with properties generally decreasing with increasing temperature. This motivates several system design considerations. The first is the selection of suitable magnet materials that can withstand the highest operating temperatures expected in a given application. This is important because heating a magnet too hot may cause permanent degradation to the magnetization. Additionally, a material with only moderate room-temperature performance may excel over other materials at higher temperatures. A second design consideration is to understand how temperature variations affect the magnetic properties and thus affect the overall system. This is critical to ensure consistent performance (or at least quantifiable temperature sensitivity) over a specified operational temperature range.

While not universally true, in many magnets, the remanence, coercivity, intrinsic coercivity, and energy product all decline with increasing temperature, as illustrated in Fig. 2 by fictitious demagnetization curves. (A counterexample to this generalization is ferrite magnets, where the coercivity can increase with temperature over a certain range [12].) Any thermally induced change may be reversible or irreversible, depending on the magnitude of temperature change.

Fig. 3 depicts an example plot of remanence versus temperature for different thermal cycles. If the magnetization returns to the original value after a thermal cycle, as indicated by curve *i* (black) in Fig. 3, the change is considered reversible. If the magnetization does not return to its original value after a thermal cycle, as indicated by curve *ii* (red) and curve *iii* (blue) in Fig. 3, the process is considered irreversible.

For a thermally demagnetized magnet, the full magnetization can usually be recovered by remagnetization with a magnetic field, so long as chemical or microstructural changes have not occurred (e.g., oxidation and phase change). Note, however, that once a magnet is installed in an application,

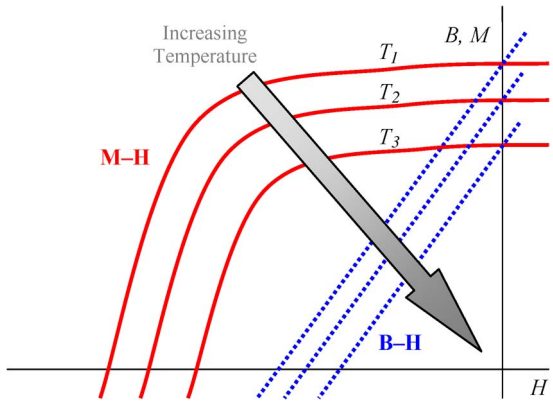

Fig. 2. General temperature dependence of M–H and B–H magnetic hysteresis loops, where $T_3 > T_2 > T_1$. The remanence, coercivity, and energy product all tend to decrease with increasing temperature.

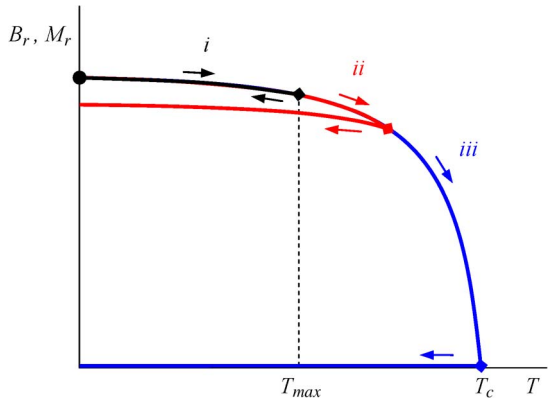

Fig. 3. Magnetization versus temperature, indicating the maximum operating temperature $T_{\max}$ and the Curie temperature T_c. Three curves are shown indicating the results of thermal cycles to increasing temperatures.

remagnetization is usually not possible. To avoid *in situ* performance degradation, magnets are often heated before installation to a level above the expected operating temperature. This "burn-in" procedure results in a one-time performance decline but ensures that the magnets remain thermally stable once in use.

The relevant thermal properties are quantified as follows. The maximum operating temperature $T_{\max}$ is defined as the temperature above which irreversible changes occur. The Curie temperature T_c is the temperature above which a magnet no longer exhibits any net magnetization. The Curie temperature is a well-defined intrinsic material property for a given compound; above it, a magnetic phase transition occurs, and the material exhibits a paramagnetic rather than ferromagnetic behavior [11]. While T_c provides an absolute upper limit for material magnetization, $T_{\max}$ is often several hundred degrees Celsius lower, and it usually sets the practical temperature limit. Below $T_{\max}$, the reversible magnetization degradation is usually quantified by the reversible temperature coefficient of remanence α (in units of percentage per degree Celsius). This value is the initial slope of the curves shown in Fig. 3, which indicates the temperature stability of a material.

D. Chemical Properties

In addition to the temperature stability, the chemical stability is a key concern for two reasons. First, in application, a magnet may be exposed to standard atmospheric conditions, so an important consideration is a magnet's propensity for oxidation, particularly when considering small magnets with high surface-area-to-volume ratios. Second, thinking ahead toward microfabricated devices, a microfabricated magnet in an integrated process flow may be subjected to numerous chemical treatments. Thus, a magnet must be able to survive short-term chemical exposure and long-term exposure to the ambient atmosphere.

Certain magnet compositions (particularly rare-earth magnets) readily oxidize in normal ambient air [12]. This oxidized layer is not strongly magnetic and thus reduces the net magnetic volume or decreases the coercivity. Protective coatings or alloy modifications are often used to increase the corrosion resistance. While the qualitative chemical stability of different alloys is widely discussed, quantitative characterization of corrosivity is less commonly reported. Where reported, the characterization of corrosion is usually performed by standard electrochemical methods measuring the corrosion potential and the corrosion current density. Additionally, oxidizing tests are usually performed in an oven at 80 °C in 80% relative humidity atmosphere and followed by a chemical analysis of the surface (e.g., energy dispersive X-ray spectroscopy or X-ray photoelectron spectroscopy) [15].

III. Bulk Hard Magnets

Before delving into microscale magnets, the well-known properties and tradeoffs of bulk permanent-magnet materials are first discussed. Macroscale hard magnets are most commonly created by powder metallurgical processes and, to a lesser degree, casting. A thorough description of permanent-magnet manufacturing can be found in [12].

To create a magnet, the desired magnetic alloy is first blended by melting appropriate quantities of the raw elements in large furnaces. To form cast magnets, the molten mixture is poured into a mold and allowed to cool. For powder-based magnets, the cooled alloy material is usually ball milled or jet milled to form fine powders. Particle sizes range from a few micrometers up to hundreds of micrometers. The powders are then pressed into molds to create a desired shape. Subsequent or simultaneous heat treatments (sintering) are used to bond the powder and also to induce precipitation, diffusion, or microstructural changes to enhance the magnetic properties. Magnetic fields can also be applied to achieve the preferred magnetic orientations (anisotropy).

Because most of the high-performance magnetic materials are brittle, the magnetic powders are often augmented with organic binders to create bonded magnets. These bonded magnets are more mechanically robust and can be formed into complex shapes using extrusion or injection molding processes. However, because of the volumetric dilution from the binder material, these bonded magnets exhibit decreased magnetic properties in comparison to fully dense sintered or cast magnets.

Common bulk permanent-magnet materials can broadly be categorized as low-energy-density ferrites (e.g., $BaFe_{12}O_{19}$ and $SrFe_{12}O_{19}$), medium-energy-density metal alloys (e.g.,

TABLE I
TYPICAL BULK HARD-MAGNET PROPERTIES

Material	Category	Bulk Manufacturing Methods	Intrinsic Coercivity H_{ci} [kA/m]	Remanence B_r [T]	Energy Product BH_{max} [kJ/m^3]	Curie Temp. T_c [°C]	Max. Op. Temp. T_{max} [°C]	Reversible Temp. Coeff. Remanence α [%/°C]	Corrosion Resistance
$MO{\cdot}6(Fe_2O_3)$	Ferrite	Powders	200-380	0.2-0.4	8-30	450-470	200-300	-0.2	Excellent
Al–Ni–Co	Metal Alloy	Cast, Powders	40-170	0.7-1.3	11-72	810-860	450-550	-0.02	Very good
$CoPt-L1_0$	Metal Alloy	Cast, Powders	360		75	840			Very good
$FePt-L1_0$	Metal Alloy	Cast, Powders	390		160	750			Very good
$SmCo_5$	Rare Earth	Powders	1300-2400	0.83-0.95	130-180	685-750	250-300	-0.04	Moderate
Sm_2Co_{17}	Rare Earth	Powders	560-2100	1.0-1.2	190-240	750-970	300-350	-0.03	Moderate
$Nd_2Fe_{14}B$	Rare Earth	Powders	880-3300	1.0-1.4	190-400	310	125-150	-0.1	Poor

Summarized from Skomski and Coey, 1999 [14] and MMPA Standard 0100-00 [16].

Al–Ni–Co, Fe–Pt, and Co–Pt alloys), and high-energy-density rare-earth alloys (e.g., $SmCo_5$, Sm_2Co_{17}, and $Nd_2Fe_{14}B$). Table I summarizes some of the more common bulk alloys and relevant material selection considerations.

A. Ferrites

Most hard ferrites have a composition of $MO \cdot 6(Fe_2O_3)$, where the metal M is usually Ba or Sr or sometimes Pb. These ceramic materials are technically ferrimagnetic, but their macroscopic behavior is similar to a ferromagnet. The material composition is usually formed by reacting a metal carbonate, e.g., $BaCO_3$, with iron oxide Fe_2O_3, e.g., to form $BaO \cdot 6(Fe_2O_3)$. From there, powder processing is the preferred manufacturing method, and both sintered and bonded ferrite magnets are commonly found. The particle size (a few micrometers for most hard ferrites) is often much smaller than the metal-alloy or rare-earth magnetic powders, since ferrites are not subject to deleterious oxidation like other common hard magnetic materials.

Ferrites usually exhibit a hexagonal crystal structure, which leads to significant uniaxial crystalline anisotropy and a large magnetic hysteresis. In spite of their relatively limited magnetic properties (remanence of $\sim$0.4 T, intrinsic coercivity of $\sim$380 kA/m, and energy product of up to $\sim$30 kJ/m^3), hard ferrites are the most commonly used general-purpose magnets because of their low cost and excellent corrosion resistance.

B. Transition Metal Alloys

Transition-metal-alloy magnets (or just "metal alloy" for brevity) employ ferromagnetic transition-metal elements of Fe, Co, and Ni with other nonferromagnetic metal elements such as Al, Pt, and Cr. Historically, ferrous steels were widespread as permanent magnets, but their magnetic properties are so low by today's standard that they are rarely considered. Metal-alloy magnets are usually manufactured by direct casting, but powder processing methods are also sometimes used.

Al–Ni–Co (often written "Alnico") magnets—alloys consisting primarily of Al, Ni, and Co with traces of Cu, Fe, and Ti—were one of the earliest high-performance hard magnets, heavily developed in the 1940s. Alnico magnets have high remanence (0.7–1.3 T) but relatively low intrinsic coercivity (40–170 kA/m). In application, the low coercivity makes them susceptible to demagnetization or remagnetization. The hard magnetic properties arise from fine rod-shaped particles precipitated from the matrix, which induce strong shape anisotropy. Al–Ni–Co magnets are not widely used today because of their low coercivity, poor mechanical properties, and relatively high cost. However, their excellent thermal stability and high Curie temperature makes them suitable for high-temperature applications. Other similar but less widely employed bulk alloys include Fe–Co–Cr and Cu–Ni–Fe, which have better ductility compared to Al–Ni–Co [2].

Binary alloys of Co–Pt and Fe–Pt have also been shown to exhibit impressive magnetic properties. The most interesting is the so-called $L1_0$ phase, which is a 50:50 composition of either Co or Fe with Pt having a face-centered tetragonal structure and exceptionally strong uniaxial crystalline anisotropy. Unfortunately, Co–Pt and Fe–Pt alloys are rarely used because of the extremely high cost of Pt. They are sometimes found in niche applications that require high corrosion resistance and good mechanical properties [14].

C. Rare-Earth Alloys

Many rare-earth lanthanide elements are ferromagnetic but with Curie temperatures well below room temperature. Rare-earth permanent magnets combine rare-earth and transition-metal elements to form compounds with strong ferromagnetic behavior at room temperature. Alloys of Sm–Co and Nd–Fe–B are the two most common commercially available rare-earth magnets, which are known for their exceptionally high magnetic strength. These magnets are almost exclusively manufactured from powders to form sintered or bonded magnets. The general weaknesses of rare-earth magnets are their susceptibility to oxidation and their relatively low operating temperatures.

Two different alloys of Sm–Co are common, i.e., $SmCo_5$ and Sm_2Co_{17}. $SmCo_5$ exhibits higher coercivity but lower remanence, whereas Sm_2Co_{17} exhibits higher remanence but lower coercivity. The energy products are up to $\sim$180 kJ/m^3 for $SmCo_5$ and $\sim$240 kJ/m^3 for Sm_2Co_{17}. Sm–Co alloys have very high Curie temperature (720 °C–900 °C), which is a benefit of the high Co content. The drawback is that Co is becoming increasingly expensive, making Sm–Co magnets more costly than their better performing Nd–Fe–B counterparts. Compared

to Nd–Fe–B, the advantage of Sm–Co alloys is better chemical stability and higher maximum operating temperature, which is generally in the range of 250 °C–350 °C. Some special alloys have been developed with for temperatures up to 550 °C [17]. Therefore, despite their relatively high cost, Sm–Co alloys find use in high-temperature high-performance applications.

Nd–Fe–B magnets (usually the alloy $Nd_2Fe_{14}B$) show the highest magnetic performance (energy product of up to 400 kJ/m^3) out of all the widely manufactured magnets. They are readily available in various shapes and sizes at relatively low cost. The primary disadvantages of Nd–Fe–B magnets are poor corrosion resistance and very low maximum operation temperature (125 °C–150 °C). The magnet surfaces are almost always coated with a metal coating (usually Ni) to limit degradation, even for room-temperature applications.

IV. Requirements for Magnetic MEMS

The application of permanent magnets at the microscale requires many considerations. Most MEMS devices and process flows are highly custom and application specific. Each system has different needs and different constraints (size, performance, temperature range, cost, process limitations, etc.). Thus, no single magnetic material or fabrication process will meet all needs. However, there are some general goals that are common to many MEMS platforms. Before delving into previously published results, it makes sense to first describe rough targets for the desired properties and to provide examples of tradeoffs in the selection of suitable magnetic materials.

A. Magnet Size

For MEMS device design, relatively large magnetic volumes are often desired to achieve large magnetic fields, magnetic forces, or electromechanical energy exchange. For example, unlike electrostatic forces, which are dependent on the surface area, magnetic forces depend on the volume. Additionally, one often-touted advantage of a magnet is the ability to create magnetic fields over fairly long distances, e.g., for actuators with large working gaps. However, the magnetic field emanating from the surface of a magnet rapidly decays with distance (e.g., the field from a magnetic dipole decays with $1/d^3$). While it is possible to achieve strong magnetic fields over relatively long distances, this requires magnets of substantial size. Typical magnet dimensions required for MEMS range from a few micrometers to hundreds of micrometers or possibly even larger, depending on the application.

B. Material Performance

For functional use, a magnet should exhibit strong magnetic properties and suitable thermal and chemical stability for the intended application. As discussed in the previous section, general material tradeoffs are well documented for bulk materials. For microscale magnets, the temperature stability and the chemical stability are generally similar to the macroscale material properties. However, the magnetic performance of microscale magnets is often lower than that in bulk, largely due to process and integration constraints (further discussed below). A decent-quality microscale magnet could be expected to have $H_{ci} > 200$ kA/m, $B_r > 0.5$ T, and $(BH)_{\max} > 30$ kJ/m^3, which is roughly the performance of a bulk ferrite magnet.

One additional consideration relating to material performance is the ability to control the direction of magnetic anisotropy either during or after deposition. Certain magnetic films and deposition processes lead to better in-plane performance, whereas others exhibit better out-of-plane performance. Isotropic materials are also possible, but these are usually of lower quality. These considerations affect material selection and the overall device design. The strength and direction of anisotropy can be influenced by the deposition temperature or postdeposition annealing, the application of magnetic fields during deposition, substrate crystallinity via lattice templating (pseudoepitaxial growth), or the material microstructure, e.g., needlelike in-plane structure versus columnlike out-of-plane structure.

Furthermore, while chemical reactivity is expected to be about the same between macroscale and microscale magnets, corrosion/oxidation effects become more important at small size scales, where surface-area-to-volume ratios become large. For example, a 50-μm-thick "skin" of oxidation may be tolerable on a 1-cm^3 magnet, but it is certainly not tolerable in a 100-μm-thick magnetic film, since half of the film would no longer be magnetic.

C. Process Integration

One of the biggest challenges for realizing microscale magnetic systems is process integration. Unlike bulk magnetic devices where magnets are separately manufactured and then assembled into the final system, microfabrication demands monolithic integration of the magnets within a multistep sequential process flow. This integrated manufacturing approach places constraints on the magnetic materials and processes that are not normally found in macroscale manufacturing.

First, wafer-level deposition processes are desired to maintain the cost, throughput, and repeatability advantages afforded by batch fabrication. As previously described, most macroscale magnets are manufactured using processes (casting and powders) that are very different from those commonly employed in microfabrication. Thus, to be suitable for microsystem integration, different processing approaches are needed.

Second, deposited micromagnets should be lithographically defined to form precise aligned geometries for device design. This requires methods for selective deposition (e.g., electroplating and screen printing) or selective etching of blanket-deposited magnetic layers. Chemical etchants for many of the complex magnetic alloys are not widely known, so selective deposition may be preferred.

Third, the magnets should be deposited at low temperatures and avoid postannealing requirements, so other integrated circuits or common MEMS materials (e.g., polymers and Al) can survive the process conditions. Ideally, room-temperature processes are preferred, but at minimum, processing temperatures should be kept below 450 °C for potential post-complimentary metal–oxide–semiconductor compatibility.

Fourth, not only should the deposition of the magnets not affect preexisting structures on a wafer, but the deposited magnets must also be stable enough to survive any subsequent processing steps (e.g., photolithography, chemical etching, plasma processes, and thermal steps).

Last, microfabricated magnets require a magnetization step after fabrication. To maintain wafer-level processing, this usually implies magnetization in only one direction. Although it is not impossible, it is difficult to magnetize magnets in different directions when they are in close proximity and share a common substrate.

All of these integration issues place strict limitations on material selection and fabrication methods, not to mention constraints on device design. For example, metal alloys can be deposited by electrodeposition or physical vapor deposition. Electroplating offers a relatively low-cost high-deposition-rate approach for achieving multimicrometer films, as well as the ability to selectively deposit material using photoresist masks. In contrast, vapor deposition is usually slower and more costly and requires postdeposition etching or polishing steps to define the pattern since standard "lift-off" methods may not work with thick layers. While electroplating may seem to be highly desirable, it requires careful control over many process parameters and often suffers from lack of repeatability. Additionally, ferrites and rare-earth magnets cannot be electrodeposited from aqueous solutions, so vapor deposition or other methods are necessary. In general, there are many tradeoffs in the selection of a material and fabrication approach.

V. Microfabricated Permanent Magnets

With a general understanding of magnetic materials and the hurdles for application at the microscale, this section now presents a review of permanent-magnet materials suitable for MEMS integration. This summary is restricted to permanent magnets that can be deposited or grown on typical MEMS substrates (e.g., Si, glass) and have film thickness values of at least 0.5 μm. This specifically excludes magnets that require manual assembly for integration, magnets on "exotic" substrates, and very thin magnetic films. The discussion is divided into two sections. Section V-A describes micromagnets fabricated using conventional thin-film microfabrication methods. Section V-B highlights "unconventional" microfabrication strategies that employ magnetic powders for the realization of micromagnets.

A. Conventionally Deposited Micromagnets

In this paper, conventional deposition encompasses physical vapor deposition [sputtering, evaporation, and pulsed-laser deposition (PLD)] and electrochemical deposition (electroplating). These wafer-level batch fabrication processes are familiar to the MEMS community and have enabled a large majority of the prior investigations into micromagnets. Table II summarizes many conventionally deposited magnets. In many cases, remanence values and energy products were not reported.

Of the various magnetic material categories, metal-alloy magnets have been the most widely studied for potential integration in MEMS, primarily because of the favorable cost, simplicity, and process integration afforded by electrodeposition. The earliest efforts for integrating permanent magnetic materials for MEMS focused on Co–Ni–X alloys, where X is normally a nonmagnetic element such as P and W. These nonmagnetic elements are usually very small in relative quantity but important. During electroplating, these elements tend to segregate at grain boundaries, forming defects that inhibit domain walls from moving, hence increasing the coercivity. However, the resulting magnetic properties are usually fairly limited. The intrinsic coercivities are usually in the range of 30–200 kA/m, and the energy products are usually less than 10 kJ/m^3 [8], [18]–[22]. Despite this modest performance, these films are readily integrated into MEMS processes using straightforward electrodeposition methods.

Motivated by the successful application in the magnetic recording area, deposition of equiatomic ordered $L1_0$ CoPt and FePt films have also been investigated. $L1_0$ refers tetragonal distortion of a face-centered cubic structure, where atomic layers of Pt are sandwiched between Fe (or Co) layers. Relatively thick films have been deposited by electroplating [23]–[25], [28], sputtering [26], and PLD [27], but high-temperature annealing (generally 400 °C–800 °C) is usually required to induce the ordered $L1_0$ structure. Intrinsic coercivities of up to 1440 kA/m [25] and energy products of up to 124 kJ/m^3 [26] have been achieved after annealing. Recently, Nakano *et al.* [27] have reported Fe–Pt thick films having the $L1_0$ phase without intentional substrate heating, although it was unclear if the substrate became hot during deposition to induce the $L1_0$ ordering. High-power PLD was used to deposit an area of 5×5 mm^2, resulting in an out-of-plane energy product of up to 105 kJ/m^3.

Another metal alloy is the Co-rich Co–Pt system, where the Co content is approximately 80% [8], [29]–[34]. This alloy offers strong magnetic properties in the as-deposited state, i.e., without any high-temperature annealing. Strong out-of-plane magnetic anisotropy is achieved by aligning the c-axis of the Co crystalline perpendicular to the substrate and encouraging a columnar microstructure with phosphorous-segregated grain boundaries. This process is enhanced by using textured seed layers, e.g., Cu (111) on Si (110), that provide a template lattice for the desired crystalline structure [30]. Wang and Arnold demonstrated 8-μm-thick patterned films with an energy product of 69 kJ/m^3 [34].

While great strides have been made with metal-alloy magnets, their properties are still fairly limited. As a result, interest has steadily grown in rare-earth magnetic materials. Since rare-earth magnets cannot be electroplated from aqueous baths, most efforts have employed sputtering or PLD. In the materials community, the magnetic properties of rare-earth thin films (< 0.5 μm) have been shown to approach that of bulk magnets. Technical challenges such as control over stoichiometry, the crystal structure, and the microstructure have been overcome, and protection layers (to mitigate oxidation and corrosion) are readily deposited on top of the magnetic films. Unfortunately, less attention has been paid to thicker films and MEMS integration issues (patterning, batch fabrication, and deposition rate). Recently, however, investigations have begun focusing

TABLE II
CONVENTIONALLY MICROFABRICATED PERMANENT MAGNETS FOR MEMS

Reference	Alloy	Fabrication Method	Integration Notes	Thickness [μm]	Intrinsic Coercivity H_{ci} [kA/m]	Remanance B_r [T]	Energy Product $(BH)_{max}$ [kJ/m^3]
Myung et al. 2003 [8]	CoNiP	Electrodeposited	None	2	75-170	--	--
Guan, Nelson 2005 [18]	CoNiP	Electrodeposited	None	1-52	55-105[a]	0.06-0.1	1.3-1.8
Liakopoulos et al. 1996 [19]	CoNiMnP	Electrodeposited	None	10-45	70-100	0.2-0.3	14
Guan, Nelson 2005 [20]	CoNiMnP	Electrodeposited	None	2-40	30-180[a]	0.01-0.1	0.3-2.6
Yufeng et al. 2005 [21]	CoNiMnP	Electrodeposited	0.2 T magnetic field	25	40-210	0.06-0.2	0.6-10
Ng et al. 2005 [22]	CoNiReWP	Electrodeposited	None	34-90	160-190	0.31-0.51	--
Rhen et al. 2003 [23]	FePt – $L1_0$	Electrodeposited	400°C anneal	0.45	240	--	--
Leistner et al. 2004 [24]	FePt – $L1_0$	Electrodeposited	600°C anneal	0.7	880	--	--
Thongmee et al. 2007 [25]	FePt – $L1_0$	Electrodeposited	400-800°C anneal	0.15-0.8	320-1440	--	--
Liu et al. 2006 [26]	FePt – $L1_0$	Sputtered	600°C anneal	6-7	446	--	124
Nakano et al. 2009 [27]	FePt– $L1_0$	PLD	small area	19-26	600	1.4	12-105
Berkh et al. 2008[28]	CoPt– $L1_0$	Electrodeposited	700°C anneal	10-16	800	0.37	--
Myung et al. 2003 [8]	CoPtP	Electrodeposited	None	1	230	0.2-0.3	--
Franz et al. 2002 [29]	CoPtW(P)	Electrodeposited	None	5-20	50-195	0.2-0.5	--
Zana et al. 2005 [30]	CoPt(P)	Electrodeposited	(110) Si substrate	2	370	0.6	52
Vieux-Rochaz et al. 2006 [31]	CoPt(P)	Electrodeposited	1.2 T magnetic field	5	225	--	--
Kulkarni, Roy 2007[32]	CoPt(P)	Electrodeposited	None	1-6	120	--	--
Berkh et al. 2007 [33]	CoPt(P)	Electrodeposited	None	40	220	0.3	--
Wang, Arnold 2008 [34]	CoPt(P)	Electrodeposited	(110) Si substrate	8	330	1.0	69
Prados et al. 1999 [35]	SmCo	Sputtered	550°C anneal	0.5	2080	--	--
Pina et al. 2005[36]	SmCo	Sputtered	450°C deposition; 550°C anneal	1.5	2100	--	--
Budde, Gatzen 2006 [37]	SmCo	Sputtered	560°C anneal; glass/alumina substrate	1-50	1200	0.7-0.75	75-90
Walther et al. 2008 [38]	SmCo	Sputtered	400 °C deposition; 750°C anneal	5	1035	0.8	140
Cadieu et al. 2001 [39]	SmCo	PLD	435°C deposition; 550°C anneal; Metal matrix	1	1200	--	--
Yamasawa et al. 2006 [40]	NdFeB/W	Sputtered	450 °C deposition;	1	800	1	53
Castaldi et al. 2006 [41]	NdFeB	Sputtered	470°C deposition	1	500-800	0.4-1.5	130-150
Dempsey et al. 2007 [42]	NdFeB	Sputtered	500°C deposition, 750°C anneal	5	1280	1.4	400
Nakano et al. 2006 [43]	NdFeB	PLD	650°C anneal; small area	120	1000	0.55	77

[a] Coercivity H_c values, not intrinsic coercivity H_{ci}.

on increasing deposition rates and developing wafer-level deposition processes with specific intent for MEMS applications [36]–[44].

Sm–Co alloys are first discussed. Prados *et al.* [35] demonstrated fairly thin (0.5 μm) sputtered Sm–Co films with a very high intrinsic coercivity of 2080 kA/m after annealing at 550 °C. Pina *et al.* [36] fabricated thicker (1.5 μm) films by sputtering Sm–Co onto a heated substrate followed by annealing at 550 °C. They reported an impressive intrinsic coercivity of 2100 kA/m, but unfortunately, no remanence or energy product was provided. Budde and Gatzen [37] sputtered Sm–Co films at deposition rates of 2.9 nm/s up to 50 μm in thickness on glass and alumina substrates. A maximum energy product of 90 kJ/m^3 was achieved for 30-μm-thick films after postdeposition annealing at 560 °C. Walther *et al.* [38] demonstrated 5-μm-thick films on silicon, which, after annealing at 750 °C, exhibited a modest intrinsic coercivity of 1035 kA/m but has a high energy product of 140 kJ/m^3. Last, in an attempt to mitigate oxidation effects, Cadieu *et al.* [39] deposited nanophase SmCo into a metal matrix using PLD. The final composite film, which was deposited at 435 °C and annealed at 550 °C, had a thickness of 1 μm and an intrinsic coercivity of 1200 kA/m.

Compared to Sm–Co, Nd–Fe–B alloys are more susceptible to oxidation, so additional coatings and protection layers are crucial. Yamasawa *et al.* [40] reported a 1-μm-thick sputtered multilayer structure with alternating layers of W and Nd–Fe–B, where the W acted to limit the oxidation of the Nd. The layers were deposited at 450 °C with resulting energy products of 50 kJ/m^3. Castaldi *et al.* [41] explored Cu and Nb buffer and cap layers on 1-μm-thick Nd–Fe–B films sputtered at 470 °C, resulting in an energy product of 150 kJ/m^3. Dempsey *et al.* [42] developed a dc triode sputtering technique to produce 5-μm-thick Nd–Fe–B thick films at deposition rates up to 5 nm/s. The reported energy product after 750 °C annealing was as high as 400 kJ/m^3, which is comparable to bulk rare-earth magnets. Nakano *et al.* [43] demonstrated extremely thick PLD Nd–Fe–B layers of up to 120 μm. However, this method has been limited to fairly small deposition areas and modest energy products (77 kJ/m^3).

While the magnetic properties of Sm–Co and Nd–Fe–B thick films are very attractive, the etching and patterning of these films remains somewhat challenging. Budde and Gatzen [37] report methods for patterning thick Sm–Co films by ion beam etching (20 nm/min) or wet chemical etching using ammonium cernitrate (12.5 μm/min). The ion milling was prohibitively

slow, and the wet etching suffered from high lateral etch rates, resulting in poor dimensional control. Walther *et al.* [44] have patterned Sm–Co and Nd–Fe–B by filling preetched trenches in the substrate, followed by chemical–mechanical planarization in a Damascene-like process. After thermal annealing, film fracture occurred on the Sm–Co films but not on the Nd–Fe–B films. Wet etching using $(NH_4)_2S_2O_8 \cdot H_2O$ and H_2SO_4 has also proved suitable for both Nd–Fe–B and Sm–Co films in the amorphous state (before annealing). Vertical sidewalls were achieved on 5-μm-thick films, with etch rates of 1.25 μm/min. However, a large lateral overetch of 20 μm was observed in both materials.

In summary, the simple Co–Ni alloys are readily integrable but fundamentally limited in performance. The better performing Fe–Pt $L1_0$ alloys and rare-earth alloys require *in situ* or postdeposition annealing at high temperatures (> 400 °C) to achieve their high magnetic properties, so the thermal budget and process integrability must be considered. The rare-earth materials have also proven to be difficult to pattern. The middle ground in performance is occupied by the Co-rich Co–Pt alloys, which exhibit good performance in the as-deposited state and are integrable via room-temperature electrodeposition.

Furthermore, with the exception of the Co–Ni–Mn alloys, which have relatively low magnetic performance, most of the better performing sputtered or electroplated films are limited to a few micrometers in thickness. This is due to intrinsic stresses that develop during deposition and/or thermal mismatch stresses that arise during annealing steps. Furthermore, the magnetic performance of a film tends to degrade with thickness due to variations in the microstructure, e.g., grain size and shape.

B. *Powder Micromagnets*

While the use of magnetic powders is ubiquitous for macroscale magnet fabrication, their use in microfabrication is certainly a foreign concept. The idea of intentionally introducing small powder particles into a "clean" environment is sure to raise eyebrows with clean-room managers. Despite the potential segregation/contamination issues, the magnetic properties of bulk-manufactured powder-based magnets are too attractive to overlook. If suitable integration methods can be developed, the complex high-temperature-material processing steps required to achieve ideal magnetic properties can be delegated to the powder manufacturing, separately from the MEMS fabrication.

Additionally, the use of magnetic powders affords the opportunity to batch fabricate magnets with thickness values that are not technologically feasible with other standard microfabrication or bulk-manufacturing methods. As previously described, sputtered or electroplated magnets are often limited to a few micrometers in thickness, while bulk-manufacturing techniques do not enable magnets much smaller than 1 mm. Thus, microscale powder processing methods may be well suited for magnets in the range of 10 μm–1 mm.

Naturally, the magnetic particle size dictates the minimum magnetic feature size. The particles must be smaller than the desired feature size to ensure a quasi-homogenous distribution of particles. Commercially available hard ferrite powders are available down to $\sim$2 μm, Sm–Co powders are available down to 5–10 μm, and Nd–Fe–B powders are available down to $\sim$50 μm. The minimum particle size is dependent on the combination of the microstructural grain size, the magnetic domain size, and thermal stability [12].

As summarized in Table III, attempts have been made to incorporate magnetic microparticles into microfabrication processes in several ways. In one approach, which was coined magnetic composite electroplating by Guan and Nelson [45], [46], nonsoluble magnetic particles were incorporated into conventional magnetic alloy electroplating baths to create metal particle composites. During deposition, the magnetic particles (e.g., $BaFe_{12}O_{19}$) were mechanically and electrochemically captured into the growing electrodeposit. So far, this approach has achieved energy densities of up to 6–9 kJ/m^3 for arrays of magnets that are 15–50 μm thick using $BaFe_{12}O_{19}$ particles in a CoNiP matrix [46].

Other approaches emulate macroscale bonded magnet powder methods using polymers/resins/inks loaded with magnetic particles. These composites can be spin coated, screen printed, or "squeegeed" into cavities to form magnets with micrometer- to millimeter-scale features. Bonded micromagnets have been achieved using ferrite, Sm–Co, and Nd–Fe–B powders in polyimide [47], epoxy [49], SU-8 [51], polymethyl-methacrylate (PMMA) [56], and resin binders [48], [50], [53]–[55]. Intrinsic coercivities of up to 900 kA/m and energy products of 24 kJ/m^3 have been achieved.

As in bulk-manufactured bonded magnets, the final magnet properties are usually weaker than those of the original magnetic powder. The coercivity generally remains constant, but the remanence is proportional to the particle fill factor, typically 60%–80% at best. This results in a lower energy density. For higher fill factors, the magnet/particle mixtures are too viscous, so screen printing and spin casting are no longer feasible.

In an attempt to overcome this fill factor limitation, Bowers *et al.* [52] demonstrated dry packing of raw Sm_2Co_{17} particles into Si trenches to form embedded micromagnets. Magnets ranging in size from 15 to 500 μm were achieved with energy densities of up to 23 kJ/m^3. A similar approach by Wang *et al.* [57] used dry packing of $Nd_2Fe_{14}B$ particles with wax particles, followed by a low-temperature heat treatment to reflow the wax and bind the particles in place. This method yielded intrinsic coercivities of up to 740 kA/m and energy products of up to 17 kJ/m^3.

VI. Conclusion

Technology development for the fabrication and integration of permanent micromagnets has steadily advanced over the past decades. The ongoing interest in micromagnetic devices has spawned a variety of investigations on materials and methods for microfabricating thick high-energy-product permanent magnets for MEMS applications.

From a size-scale perspective, conventionally deposited (sputtered, electroplated, and PLD) micromagnets have demonstrated excellent magnetic performance but are limited in

TABLE III
POWDER-BASED PERMANENT MAGNETS FOR MEMS

Reference	Magnetic Powder	Carrier Material	Fabrication Method	Thickness [μm]	Intrinsic Coercivity H_{ci} [kA/m]	Remanance B_r [T]	Energy Product $(BH)_{max}$ [kJ/m^3]
Guan et al. 2004 [45]	$BaFe_{12}O_{19}$	Ni	MCE[a]	5	24-170[b]	0.16-0.22	1-2
Guan et al. 2004 [45]	$BaFe_{12}O_{19}$	Ni	MCE	5	13-30[b]	0.17-0.27	0.6-1
Guan et al. 2004 [45]	$BaFe_{12}O_{19}$	CoNiMnP	MCE	5	76-160[b]	0.2-0.25	7-8
Guan, Nelson 2006 [46]	$BaFe_{12}O_{19}$	CoNiP	MCE	15-50	120-175	0.2-0.25	6-9
Lagorce, Allen 1997 [47]	$SrFe_{12}O_{19}$	Polyimide	Spin-casting	10-20	320	0.16-0.28	5-12
Yuan et al. 2002 [48]	$SrFe_{12}O_{19}$	Resin	Screen-printing	8-15	160-320	--	--
Cho, Ahn 2003 [49]	$SrFe_{12}O_{19}$	Epoxy resin	Squeegee	60-70	350-360	0.03	2-3
Rozenberg et al. 2006 [50]	$SrFe_{12}O_{19}$	Resin	Screen-printing	10-220	480	0.4	24
Dutoit et al. 1999 [51]	Sm_2Co_{17}	SU-8	Spin-casting	15	140-550	0.25-0.34	22
Bowers et al. 2007 [52]	Sm_2Co_{17}	none	Dry-packing	15-500	130-140	0.3-0.5	18-23
Pawlowski et al. 2003 [53]	$Nd_2Fe_{14}B$	Resin	Tape-casting	100-800	300-800	0.35-0.45	--
Pawlowski, Töpfer 2004 [54]	$Nd_2Fe_{14}B$	Resin	Screen-printing	10-50	300-900	0.2-0.4	--
Schwarzer et al. 2004 [55]	$Nd_2Fe_{14}B$	Resin	Screen-printing	10-50	800	0.4-0.5	--
Guan, Nelson 2004 [45]	$Nd_2Fe_{14}B$	NiP	MCE	5-20	50-190[b]	0.24-0.35	2-3
Romero et al. 2006 [56]	$Nd_2Fe_{14}B$	PMMA	"Rain-dropping"	500	1090	0.25-0.7	--
Wang et al. 2008 [57]	$Nd_2Fe_{14}B$	Wax particles	Dry-packing	320	720-740	0.22-0.34	8-17

[a] MCE = magnetic composite electroplating
[b] Coercivity H_c values, not intrinsic coercivity H_{ci}.

thickness to ~100 μm. Powder-based fabrication methods appear to be filling a niche for magnets in the size range of 10 μm–1 mm, but their properties have been limited by the availability of magnetic powders and nonideal fabrication strategies.

From a magnetic property perspective, the best performing micromagnets have been achieved using conventionally deposited rare-earth alloys. Unfortunately, the high performers are hampered by requirements for special substrates, high-temperature annealing, or other integration issues, which preclude their widespread adoption. The best performing sputtered Nd–Fe–B magnets have approached the theoretical performance limits currently known for magnetic materials but require high-temperature annealing and specialized deposition systems. Where high temperatures are not permissible, Co-rich Co–Pt alloys offer good magnetic performance and are highly integrable via electrodeposition methods. Last, while powder-based micromagnets are relatively immature and have so far been limited in performance, the ability to realize thick magnetic structures at low temperatures and low cost makes them very appealing. There are many opportunities for enhancing the processes and properties of these powder-based magnets, so they may become more prominent in time.

From an integration perspective, many of the superb magnetic properties described above were obtained under ideal conditions, without explicit consideration for integration into a MEMS device process. Examples of process incompatibilities include using high-pH electroplating solutions at elevated temperatures, which will dissolve standard photoresist masks; requiring nonstandard substrate materials or specific crystalline orientations, which limits versatility; requiring *in situ* or post-deposition heat treatments, which exceed the temperature limits of other common MEMS materials; and lacking means for photolithographic patterning. Clearly, if these magnetic films are to be integrated into more complex micromachined MEMS transducers, these integration issues must be resolved.

Additionally, the process compatibility and long-term stability of these films with regard to predeposition and postdeposition thermal cycling, chemical exposure, mechanical stress, etc., are largely unknown. Systematic characterization of long-term thermal and chemical stability is a fairly mundane research task but is of critical importance. The stability of any micromagnetic material must be well understood for application in any viable commercial end product.

In conclusion, while great strides have been made over the last decade to develop suitable permanent-magnet materials, there are still many opportunities for advancements. As in bulk materials, there is no "silver bullet" process or material that can satisfy all performance needs for all applications. Magnetic materials and their application in MEMS remains an active and interesting area for research and development.

REFERENCES

[1] O. Cugat, J. Delamare, and G. Reyne, "Magnetic micro-actuators and systems (MAGMAS)," *IEEE Trans. Magn.*, vol. 39, no. 5, pp. 3607–3612, Nov. 2003.
[2] R. C. O'Handley, *Modern Magnetic Materials, Principles, and Applications*. New York: Wiley-Interscience, 2000.
[3] P. J. Grundy, "Thin film magnetic recording media," *J. Phys. D, Appl. Phys.*, vol. 31, no. 21, pp. 2975–2990, Nov. 1998.
[4] D. Weller, "Extremely high-density longitudinal magnetic recording media," *Annu. Rev. Mater. Sci.*, vol. 30, pp. 611–644, 2000.
[5] J. Judy, "Microelectromechanical systems (MEMS): Fabrication, design and applications," *Smart Mater. Struct.*, vol. 10, no. 6, pp. 1115–1134, Dec. 2001.
[6] E. I. Cooper, C. Bonhôte, J. Heidmann, Y. Hsu, P. Kern, J. W. Lam, M. Ramasubramanian, N. Robertson, L. T. Romankiw, and H. Xu, "Recent developments in high-moment electroplated materials for recording heads," *IBM J. Res. Develop.*, vol. 49, no. 1, pp. 103–126, Jan. 2005.
[7] J. W. Judy and N. Myung, "Magnetic materials for MEMS," in *Proc. MRS Workshop MEMS Mater.*, San Francisco, CA, Apr. 5–6, 2002, pp. 23–26.
[8] N. V. Myung, D.-Y. Park, B.-Y. Yoo, and P. T. A. Sumodjo, "Development of electroplated magnetic materials for MEMS," *J. Magn. Magn. Mater.*, vol. 265, no. 2, pp. 189–198, Sep. 2003.

[9] D. Niarchos, "Magnetic MEMS: Key issues and some applications," *Sens. Actuators A, Phys.*, vol. 109, no. 1/2, pp. 166–173, Dec. 2003.
[10] T.-S. Chin, "Permanent magnet films for applications in microelectromechanical systems," *J. Magn. Magn. Mater.*, vol. 209, no. 1–3, pp. 75–79, Feb. 2000.
[11] B. D. Cullity and C. D. Graham, *Introduction to Magnetic Materials*. London, U.K.: Oxford Univ. Press, 2008.
[12] P. Campbell, *Permanent Magnet Materials and Their Application*. Cambridge, U.K.: Cambridge Univ. Press, 1994.
[13] E. P. Furlani, *Permanent Magnet and Electromechanical Devices: Materials, Analysis and Applications*. New York: Academic, 2001.
[14] R. Skomski and J. M. D. Coey, *Permanent Magnetism*. Bristol, U.K.: Inst. Phys. Pub., 1999.
[15] M. Yue, J. X. Zhang, W. Q. Liu, and G. P. Wang, "Chemical stability and microstructure of Nd–Fe–B magnet prepared by spark plasma sintering," *J. Magn. Magn. Mater.*, vol. 271, no. 2/3, pp. 364–368, May 2004.
[16] Magnetic Materials Producers Association, Standard Specifications for Permanent Magnet Materials, 2000. [Online]. Available: http://www.intl-magnetics.org
[17] Ultra-High Temperature Samarium Cobalt Magnets product datasheets: Electron Energy Corp. [Online]. Available: http://www.electronenergy.com/products/samarium-cobalt-uht.htm
[18] S. Guan and B. J. Nelson, "Pulse-reverse electrodeposited nanograinsized CoNiP thin films and microarrays for MEMS actuators," *J. Electrochem. Soc.*, vol. 152, no. 4, pp. C190–C195, 2005.
[19] T. M. Liakopoulos, W. Zhang, and C. H. Ahn, "Micromachined thick permanent magnet arrays on silicon wafers," *IEEE Trans. Magn.*, vol. 32, no. 5, pp. 5154–5156, Sep. 1996.
[20] S. Guan and B. J. Nelson, "Electrodeposition of low residual stress CoNiMnP hard magnetic thin films for magnetic MEMS actuators," *J. Magn. Magn. Mater.*, vol. 292, pp. 49–58, Apr. 2005.
[21] Y. Su, H. Wang, G. ding, F. Cui, W. Zhang, and W. Chen, "Electroplated hard magnetic materials and its application in microelectromechanical systems," *IEEE Trans. Magn.*, vol. 41, no. 12, pp. 4380–4383, Dec. 2005.
[22] W. B. Ng, A. Takada, and K. Okada, "Electrodeposited Co-Ni-Re-W-P thick array of high vertical magnetic anisotropy," *IEEE Trans. Magn.*, vol. 41, no. 10, pp. 3886–3888, Oct. 2005.
[23] F. M. F. Rhen, G. Hinds, C. O'Reilly, and J. M. D. Coey, "Electrodeposited FePt films," *IEEE Trans. Magn.*, vol. 39, no. 5, pp. 2699–2701, Sep. 2003.
[24] K. Leistner, J. Thomas, H. Schlörb, M. Weisheit, L. Schultz, and F. Fähler, "Highly coercive electrodeposited FePt film by postannealing in hydrogen," *Appl. Phys. Lett.*, vol. 85, no. 16, pp. 3498–3500, Oct. 2004.
[25] S. Thongmee, J. Ding, J. Y. Lin, D. J. Blackwood, J. B. Yi, and J. H. Yin, "FePt films fabricated by electrodeposition," *J. Appl. Phys.*, vol. 101, no. 9, p. 09K519, May 2007.
[26] W. F. Liu, S. Suzuki, D. S. Li, and K. Machida, "Magnetic properties of Fe–Pt thick-film magnets prepared by RF sputtering," *J. Magn. Magn. Mater.*, vol. 302, no. 1, pp. 201–205, Jul. 2006.
[27] M. Nakano, S. Shibata, T. Yanai, and H. Fukunaga, "Anisotropic properties in Fe–Pt thick film magnets," *J. Appl. Phys.*, vol. 105, no. 7, p. 07A732, Mar. 2009.
[28] O. Berkh, Y. Rosenberg, Y. S. Diamand, and E. Gileadi, "Electrodeposited near-equiatomic CoPt thick films," *Electrochem. Solid-State Lett.*, vol. 11, no. 4, pp. D38–D41, 2008.
[29] S. Franz, M. Bestetti, M. Consonni, and P. L. Cavallotti, "Electrodeposition of micromagnets of CoPtW(P) alloys," *Microelectron. Eng.*, vol. 64, no. 1–4, pp. 487–494, Oct. 2002.
[30] I. Zana, G. Zangari, and M. Shamsuzzoha, "Enhancing the perpendicular magnetic anisotropy of Co–Pt(P) films by epitaxial electrodeposition onto Cu(111) substrates," *J. Magn. Magn. Mater.*, vol. 292, pp. 266–280, Apr. 2005.
[31] L. Vieux-Rochaz, C. Dieppedale, B. Desloges, D. Gamet, C. Barragatti, H. Rostaing, and J. Meunier-Carus, "Electrodeposition of hard magnetic CoPtP materials and integration into magnetic MEMS," *J. Micromech. Microeng.*, vol. 16, no. 2, pp. 219–224, Feb. 2006.
[32] S. Kulkarni and S. Roy, "Development of nanostructured, stress-free Co-rich CoPtP films for magnetic microelectromechanical system applications," *J. Appl. Phys.*, vol. 101, no. 9, p. 09K524, May 2007.
[33] O. Berkh, Y. Rosenberg, Y. S. Diamand, and E. Gileadi, "Deposition of CoPtP films from citric electrolyte," *Microelectron. Eng.*, vol. 84, no. 11, pp. 2444–2449, Nov. 2007.
[34] N. Wang and D. P. Arnold, "Thick electroplated Co-rich Co–Pt micromagnet arrays for magnetic MEMS," *IEEE Trans. Magn.*, vol. 44, no. 11, pp. 3969–3972, Nov. 2008.
[35] C. Prados, A. Hernando, G. C. Hadjipanayis, and J. M. Gonzalez, "Coercivity analysis in sputtered Sm–Co thin films," *J. Appl. Phys.*, vol. 85, no. 8, pp. 6148–6150, Apr. 1999.
[36] E. Pina, F. J. Palomares, M. A. Garcia, F. Cebollada, A. de Hoyos, J. J. Romero, A. Hernando, and J. M. Gonzalez, "Coercivity in SmCo hard magnetic films for MEMS application," *J. Magn. Magn. Mater.*, vol. 290/291, pp. 1234–1236, Apr. 2005.
[37] T. Budde and H. H. Gatzen, "Thin film Sm–Co magnets for use in electromagnetic microactuators," *J. Appl. Phys.*, vol. 99, no. 8, p. 08N304, Apr. 2006.
[38] A. Walther, D. Givord, N. M. Dempsey, K. Khlopkov, and O. Gutfleisch, "Structural, magnetic, and mechanical properties of 5 μm thick SmCo films suitable for use in microelectromechanical systems," *J. Appl. Phys.*, vol. 103, no. 4, p. 043911, Feb. 2008.
[39] F. J. Cadieu, L. Chen, and B. Li, "Enhanced magnetic properties of nanophase $SmCo_5$ film dispersions," *IEEE Trans. Magn.*, vol. 37, no. 4, pp. 2570–2572, Jul. 2001.
[40] K. Yamasawa, X. Liu, and A. Morisako, "Nd–Fe–B films with perpendicular magnetic anisotropy," *J. Appl. Phys.*, vol. 99, no. 8, p. 08N302, Apr. 2006.
[41] L. Castaldi, M. R. F. Gibbs, and H. A. Davies, "Effect of the target power and composition on RE-Fe-B thin films with Cu and Nb buffer and cap layers," *J. Appl. Phys.*, vol. 100, no. 9, p. 093904, Nov. 2006.
[42] N. M. Dempsey, A. Walther, F. May, D. Givord, K. Khlopkov, and O. Gutfleisch, "High performance hard magnetic Nd–Fe–B thick films for integration into micro-electro-mechanical systems," *Appl. Phys. Lett.*, vol. 90, no. 9, p. 092509, Mar. 2007.
[43] M. Nakano, S. Sato, H. Fukunaga, and F. Yamashita, "A method of preparing anisotropic Nd–Fe–B film magnets by pulsed laser deposition," *J. Appl. Phys.*, vol. 99, no. 8, p. 08N301, Apr. 2006.
[44] A. Walther, C. Marcoux, B. Desloges, R. Grechishkin, D. Givord, and N. M. Dempsey, "Micro-patterning of NdFeB and SmCo magnet films for integration into micro-electro-mechanical-systems," *J. Magn. Magn. Mater.*, vol. 321, no. 6, pp. 590–594, Mar. 2009.
[45] S. Guan, B. J. Nelson, and K. Vollmers, "Electrochemical codeposition of magnetic particle-ferromagnetic matrix composites for magnetic MEMS actuator applications," *J. Electrochem. Soc.*, vol. 151, no. 9, pp. C545–C549, 2004.
[46] S. Guan and B. J. Nelson, "Magnetic composite electroplating for depositing micromagnets," *J. Microelectromech. Syst.*, vol. 15, no. 2, pp. 330–337, Apr. 2006.
[47] L. K. Lagorce and M. G. Allen, "Magnetic and mechanical properties of micromachined strontium ferrite/polyimide composite," *J. Microelectromech. Syst.*, vol. 6, no. 4, pp. 307–312, Dec. 1997.
[48] Z. C. Yuan, A. J. Williams, T. C. Shields, S. Blackburn, C. B. Ponton, J. S. Abell, and I. R. Harris, "The production of Sr hexaferrite thick films by screen printing," *J. Magn. Magn. Mater.*, vol. 247, no. 3, pp. 257–269, Jun. 2002.
[49] H. J. Cho and C. H. Ahn, "Microscale resin-bonded permanent magnets for magnetic micro-electro-mechanical systems applications," *J. Appl. Phys.*, vol. 93, no. 10, pp. 8674–8676, May 2003.
[50] Y. I. Rozenberg, Y. Rosenberg, V. Krylov, G. Belitsky, and Y. S. Diamand, "Resin-bonded permanent magnetic films with out-of-plane magnetization for MEMS applications," *J. Magn. Magn. Mater.*, vol. 305, no. 2, pp. 357–360, Oct. 2006.
[51] B. M. Dutoit, P. A. Bese, H. Blanchard, L. Guérin, and R. S. Popovich, "High performance micromachined Sm_2Co_{17} polymer bonded magnets," *Sens. Actuators A, Phys.*, vol. 77, no. 3, pp. 178–182, Nov. 1999.
[52] B. J. Bowers, J. S. Agashe, and D. P. Arnold, "A method to form bonded micromagnets embedded in silicon," in *Proc. 14th Int. Conf. Solid-State Sens., Actuators, Microsyst. (TRANSDUCERS)*, Lyon, France, Jun. 2007, vol. 2, pp. 1581–1584.
[53] B. Pawlowski, S. Schwarzer, A. Rahmig, and J. Töpfer, "NdFeB thick films prepared by tape casting," *J. Magn. Magn. Mater.*, vol. 265, no. 3, pp. 337–344, Oct. 2003.
[54] B. Pawlowski and J. Töpfer, "Permanent magnetic Nd–Fe–B thick films," *J. Mater. Sci.*, vol. 39, no. 4, pp. 1321–1324, Feb. 2004.
[55] S. Schwarzer, B. Pawlowski, A. Rahmig, and J. Töpfer, "Permanent magnetic thick films from remanence optimized NdFeB-inks," *J. Mater. Sci.*, vol. 15, no. 3, pp. 165–168, Mar. 2004.
[56] J. J. Romero, R. Cuadrado, E. Pina, A. de Hoyos, F. Pigazo, F. L. Palomares, A. Hernando, R. Sastre, and J. M. Gonzalez, "Anisotropic polymer bonded hard-magnetic films for micro-electromechanical system applications," *J. Appl. Phys.*, vol. 99, no. 8, p. 08N303, Apr. 2006.
[57] N. Wang, B. Bowers, and D. P. Arnold, "Wax-bonded NdFeB micromagnets for microelectromechanical systems application," *J. Appl. Phys.*, vol. 103, pp. 07E109-1–07E109-3, Apr. 2008.

David P. Arnold (S'97–M'04) received dual B.S. degrees in electrical and computer engineering and the M.S. degree in electrical engineering from the University of Florida (UF), Gainesville, in 1999 and 2001, respectively, and the Ph.D. degree in electrical engineering from the Georgia Institute of Technology, Atlanta, in 2004. During his graduate studies, he held research fellowships from the National Science Foundation and the Tau Beta Pi Engineering Honor Society.

He is currently an Assistant Professor in the Department of Electrical and Computer Engineering, UF. His research focuses on the design, fabrication, and characterization of magnetically based microsensors/microactuators, as well as miniaturized power and energy systems.

Dr. Arnold is an active participant in the magnetics and MEMS communities, serving on various conference committees for the MEMS, Hilton Head, Transducers, Sensors, MMM, and Intermag meetings. He is the Technical Program Cochair of the 2009 International Workshop on Micro and Nanotechnology for Power Generation and Energy Conversion Applications (PowerMEMS). He is a recipient of the 2008 Presidential Early Career Award in Science and Engineering (PECASE) and the 2009 DARPA Young Faculty Award. He is the current UF Chapter Faculty Advisor and a member of the Eta Kappa Nu ECE Engineering Honor Society. He is also a member Tau Beta Pi and the American Society for Engineering Education.

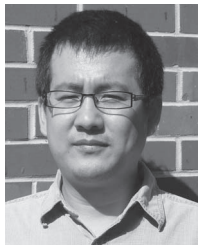

Naigang Wang (S'07) received the B.S. degree in materials science and engineering from Jilin University, Changchun, China, in 1999, and the M.S. degree in materials science and engineering from the Virginia Polytechnic Institute and State University, Blacksburg, in 2005. He is currently working toward the Ph.D. degree in materials science and engineering at the University of Florida, Gainesville.

His research focuses on the integration of magnetic materials into MEMS transducers such as magnetic energy harvesters and magnetic microactuators.